Современный статус вычислений формфакторов мезонов в решеточной КХД

Виталий Борняков

НИЦ "Курчатовский Институт" - ИФВЭ, Протвино

Физика частиц при средних и высоких энергиях
ИФВЭ, Протвино, 2-5.06.2026

Цель:

Показать, что решеточная регуляризация КХД (РКХД)

1) Является теоретически корректной
2) Позволяет вычислять многие физические величины с контролируемой точностью
3) Точность вычислений феноменологически важных физических величин достигла O(1%)
4) Пример таких физических величин - мезонные формфакторы в распадах заряженных псевдоскалярных мезонов $P_{l2}(\gamma), P_{l3}(\gamma)$
5) Результаты экспериментов Istra+ и OKA вызывают интерес, в частности у сообщества физиков-теоретиков, выполняющих исследования в РКХД.

The numerical simulations of Lattice QCD (LQCD) allowed an unpreceded progress in understanding the non-perturbative dynamics of strong interactions. Precise calculations of the hadron spectrum and accurate predictions of hadronic matrix elements are now a reality and more and more quantities relevant to the phenomenology of the Standard Model and for searches of signals of new physics beyond the SM will soon become available.
This progress has been possible thanks to the development of very sophisticated theoretical tools coupled to an extraordinary increase of the computer power and memory.

Guido Martinelli, 2023

Plan

1. Introduction: Lattice QCD
2. Two-point and three-point correlators
3. Leptonic and semileptonic psudoscalar mesons decays
4. Conclusions

Lattice regularization of QCD (K. Wilson, 1974)

- definition of QCD beyond perturbation theory i.e., it is well defined at any coupling

Problem: Euclidean space

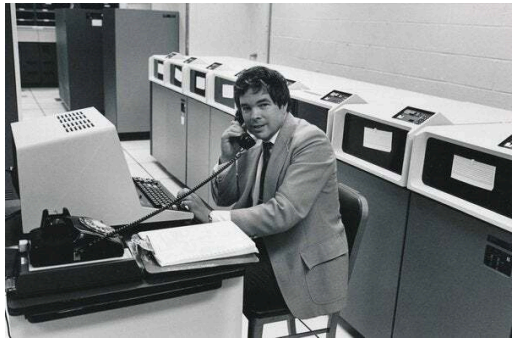

PHYSICAL REVIEW D VOLUME 10, NUMBER 8 15 OCTOBER 1974

Confinement of quarks*

Kenneth G. Wilson

Laboratory of Nuclear Studies, Cornell University, Ithaca, New York 14850

(Received 12 June 1974)

A mechanism for total confinement of quarks, similar to that of Schwinger, is defined which requires the existence of Abelian or non-Abelian gauge fields. It is shown how to quantize a gauge field theory on a discrete lattice in Euclidean space-time, preserving exact gauge invariance and treating the gauge fields as angular variables (which makes a gauge-fixing term unnecessary). The lattice gauge theory has a computable strong-coupling limit; in this limit the binding mechanism applies and there are no free quarks. There is unfortunately no Lorentz (or Euclidean) invariance in the strong-coupling limit. The strong-coupling expansion involves sums over all quark paths and sums over all surfaces (on the lattice) joining quark paths. This structure is reminiscent of relativistic string models of hadrons.

Lattice QCD

Frank Wilczek, 2003, Opportunities, challenges, and fantasies in lattice QCD:

"A major triumph of lattice QCD is already enshrined in the PDG"

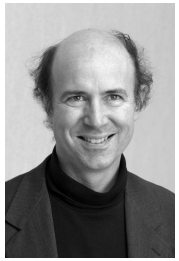

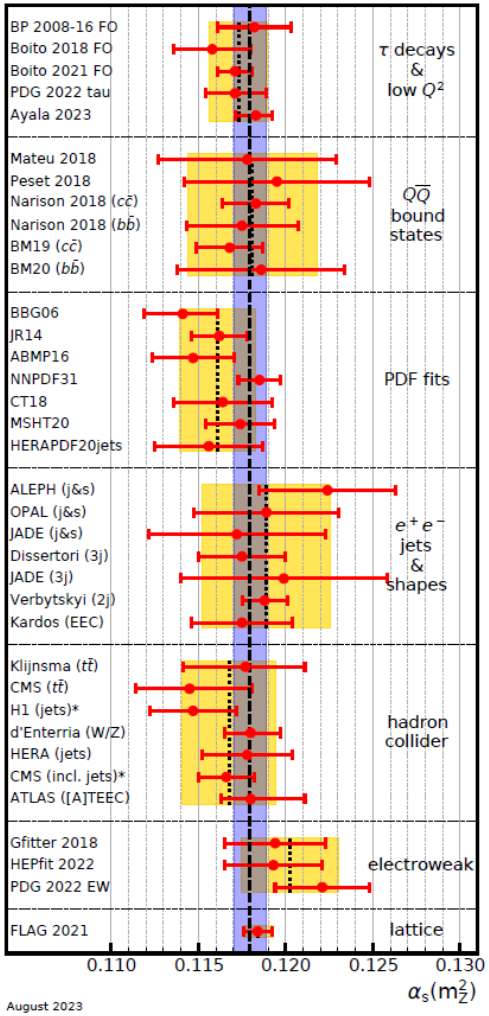

Figure 9.2: Summary of determinations of $\alpha_s(m_Z^2)$ with uncer-

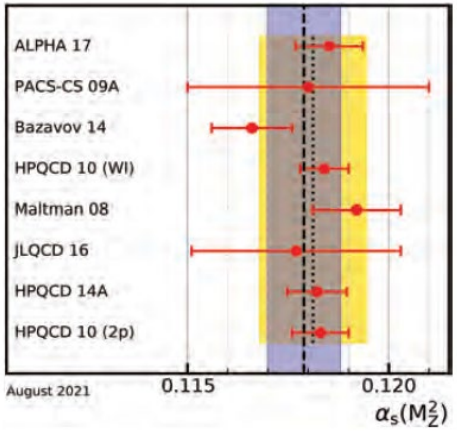

Figure 9.5: Lattice determinations that enter the FLAG2019 average. The yellow (light shaded) band and dotted line indicates the average value for this sub-field. The dashed line and blue (dark shaded) band represent the final world average value of $\alpha_s(M_Z^2)$.

Lattice QCD

Frank Wilczek, 2024, QCD at 50: Golden Anniversary, Golden Insights, Golden Opportunities

"Today, after decades of heroic work from the lattice gauge theory community, we have calculations of the low-lying spectrum that agree in full detail with experimental measurements, at the few percent level"

David Gross, 2016, Quantum Chromodynamics – The perfect Yang Mills gauge field theory:

"Lattice QCD remains, so far, the only tool for precise, controllable, first principle calculations of large scale hadronic properties. Lattice QCD has been enormously successful, reaching a new level of maturity due to Moore's Law and to theoretical ingenuity... We can now calculate, from first principles and with controllable errors, to one percent or better, the mass spectrum of all of the particles that were being discovered when I was a graduate student. To a theorist this is enormously pleasing."

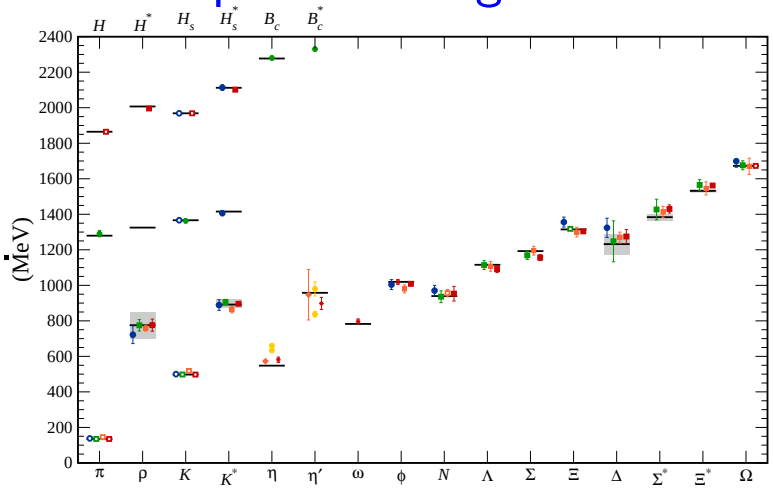

Lattice regularization

'Only recently has the combination of powerful supercomputers, sophisticated numerical techniques, and advanced theoretical approaches allowed, for the first time, the computation of physical quantities at phenomenologically relevant accuracy'
50 Years of Quantum Chromodynamics, Eur.Phys.J.C 83 (2023) 1125
'In the last decade, simulations directly at the physical isospin-symmetric light quark masses have become standard, removing the need for a chiral extrapolation and thus **significantly reducing the overall error**. The present frontier, is the inclusion of isospin breaking. This will be needed to push the accuracy of calculations below the percent level.'
REVIEW OF PARTICLE PHYSICS, Particle Data Group, 2024

Lattice regularization

Lattice QCD is obtained by replacing the four-dimensional space-time continuum with a hypercubic lattice and by restricting the quark and gauge fields to the lattice sites and links. The lattice provides a regularization of the ultra-violet divergences. The lattice QCD is, therefore, mathematically well defined.

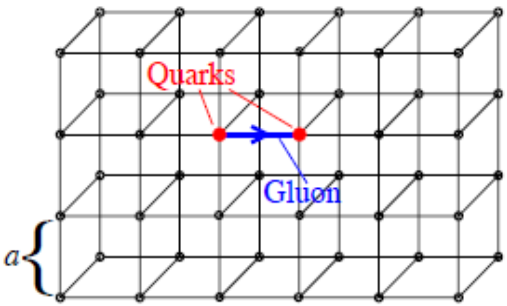

$$U_\mu(x) \;=\; P\exp\left(i\int_{C_{x,x+a\hat{\mu}}} gA_\mu(s)ds\right) \approx 1 + iagA_\mu(x) + O(a^2)\,;\; U_\mu(x) \;\in\; SU(3)$$

$$S_W \;=\; \beta \sum_{x,\mu<\nu}(1 - \tfrac{1}{N_c}\mathrm{ReTr}U_{\mu\nu}) \;=\; a^4\left(\frac{\beta}{2N_c}\sum_{x,\mu<\nu}\mathrm{Tr}[F^2_{\mu\nu}] + O(a^2)\right)$$

$$\beta \;=\; \frac{2N_c}{g^2}$$

$$S_F = \sum_{x,y}\bar{\psi}_x M_{xy}(U)\psi_y$$

M_{xy} - massive lattice Dirac operator,
a matrix with coordinate, spin, color, and flavor indices;
$\bar{\psi}_x, \psi_y$ - anticommuting Grassmann variables defined
at each site of the lattice; belong to the fundamental representation of $SU(3)$

Lattice regularization, cont.

$$\langle O(U,\bar{\psi},\psi\rangle = \frac{1}{Z}\int \mathscr{D}U\ e^{-S_G(U)}\det M(U)\ O(U,M^{-1}(U))$$

Integral of finite dimensionality. Importance sampling

$$P\{U\} \propto e^{-S_{eff}(U)}\,, \qquad S_{eff}(U) = S_G(U) - \log(\det M(U))$$

Markov chains, Monte Carlo algorithms,
Hybrid Monte Carlo = Molecular dynamics + Monte Carlo.
Important numerical task - inversion $M^{-1}_{xy}(U)$
There is no problem of gauge fixing

Lattice regularization, cont.

Sources of errors:

- statistical error (depends on number of independent configurations of gauge field)
- extrapolation $a \to 0$
- extrapolation $m_\pi \to m_{\pi,phys}$ (mostly solved)
- finite volume effects ($m_\pi L \gtrsim 4$, i.e. $L \gtrsim 5$fm

Lattice regularization, cont.

Input parameters (dimensionless):

- lattice coupling $\beta = 6/g^2$; $a = a(\beta)$; increasing $\beta \rightarrow$ decreasing a

to determine a in physical units: hadron mass, e.g. m_Ω:
$m_\Omega^{latt} = a\ m_\Omega$

- light quark mass $am_u = am_d \equiv am_l$ (isospin symmetry); m_π, f_π, m_N
- s-quark mass am_s; m_K, f_K
- c-quark mass am_c; m_{D_s}
- b-quark mass am_b; m_{B_s} or m_Υ (Note: b-quark is usually treated only as a valence quark

All other quantities are pre/post dictions that can be compared to experiment

Present day calculations are increasingly done with physical or near physical values of m_l, requiring at most only a short extrapolation or interpolation.

Physical observables

- running coupling $\alpha_s(q)$
- hadron masses
- decay constants
- semileptonic formfactors
- quark masses
- nucleon matrix elements
- kaon mixing

2003-2005: first ``realistic" lattice QCD results

based on simulations with three flavors of sea quarks ($n_f = 2 + 1$):

C. Davies et al [HPQCD, MILC, Fermilab Lattice, hep-lat/0304004, 2004 PRL]

A. Kronfeld et al [Fermilab Lattice, MILC, HPQCD, hep-lat/0509169,Int.J.Mod.Phys 2006]

Quenched QCD

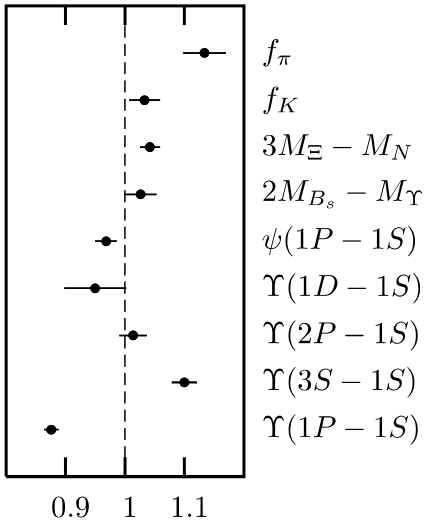

full QCD

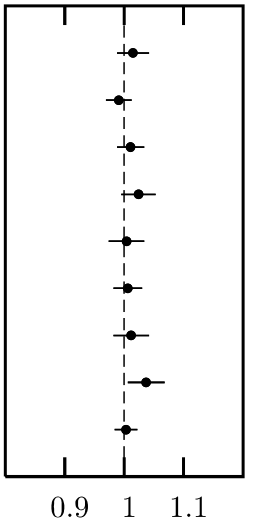

First lattice QCD *predictions*, confirmed by experiment:

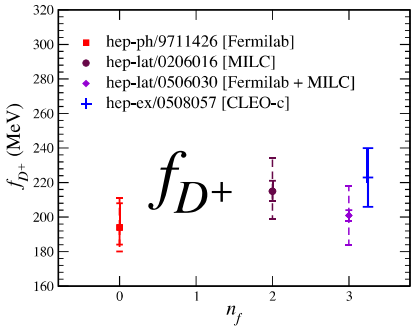

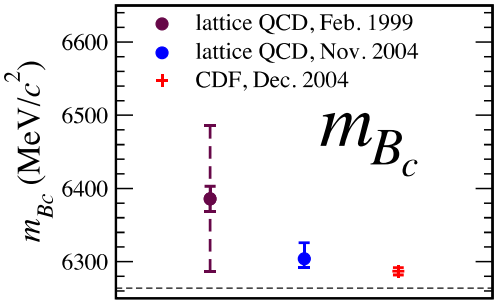

shape of form factor

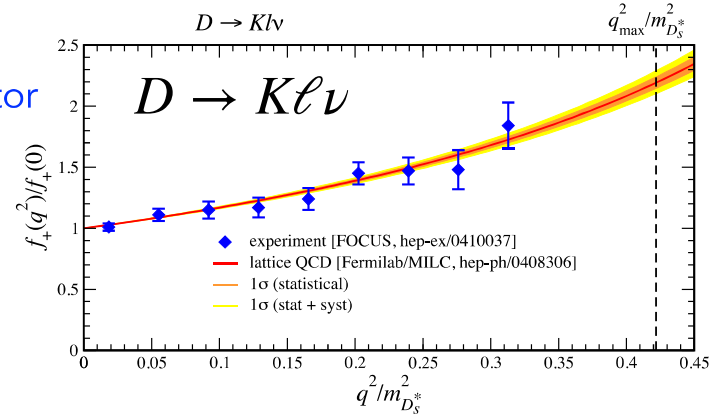

Two-point correlators

$$C_{2\mathrm{pt.}}(t) \equiv \langle O(t)\, O^\dagger(0)\rangle,$$

$O(t)$ is a generic operator with the quantum numbers of a state we wish to study

$O(t) = e^{\hat{H}t} O(0)\, e^{-\hat{H}t}, \qquad \hat{H}$ - QCD Hamiltonian

$$C_{2\mathrm{pt.}}(t) = \sum_n |\langle 0|O(0)|E_n\rangle|^2\, e^{-E_n t},$$

$$C_{2\mathrm{pt.}}(t) \approx |\langle 0|O(0)|E_0\rangle|^2\, e^{-E_0 t},$$

where corrections scale as $e^{-(E_1-E_0)\,t}$

We extract ground state energy (mass for $\vec{p}=0$) E_0 and matrix element $|\langle 0|O(0)|E_0\rangle|$

Two-point correlators

As example, interpolating operator for π^+ is
$\pi^+(x) = \bar{d}(x)\gamma_5 u(x)$,
where u is the up-quark field and d is the down-quark field.

$$C_{2\mathrm{pt.},\pi^+}(t) = -\langle \sum_{\mathrm{x}} \mathrm{Tr}\left[M_u^{-1}(\mathrm{x}, t; 0, 0)\, \gamma_5\, M_d^{-1}(0, 0; \mathrm{x}, t)\, \gamma_5 \right] \rangle \quad (1)$$

Here, M_f^{-1} denotes the quark propagator for flavor f,

Three-point correlators

Three-point correlation functions allow the extraction of matrix elements of operators. Such matrix elements are key to computing QCD contributions to electroweak decays and electromagnetic form factors, among many different quantities.

$$C_{3\mathrm{pt}}(t, t_c) = \langle 0|O(t)\,\mathscr{J}(t_c)O^\dagger(0)|0\rangle,$$

where $\mathscr{J}$ is the operator which matrix elements we want to determine. In some special cases, this is a conserved current.
The spectral decomposition of $C_{3\mathrm{pt}}$

$$C_{3\mathrm{pt}}(t, t_c) = \sum_{n,m} \langle 0|O(0)|E_n\rangle\langle E_n|\mathscr{J}(0)|E_m\rangle\langle E_m|O^\dagger(0)|0\rangle\, e^{-E_n(t-t_c)}\, e^{-E_m t_c}.$$

At large t_c and $t - t_c$, the ground-state matrix element

$$C_{3\mathrm{pt}}(t, t_c) = |\langle 0|O(0)|E_0\rangle|^2 e^{-E_0 t}\underline{\langle E_0|\mathscr{J}(0)|E_0\rangle}$$

dominates, allowing for the extraction of physical observables such as form factors and decay constants. Careful analysis is required to isolate the desired contributions and control excited-state contamination.

Leptonic and semileptonic meson decay

The Cabibbo-Kobayashi-Maskawa (CKM) matrix elements in the first row V_{ud}, V_{us}, V_{ub} are important for checks of the Standard Model. The kaon leptonic (K_{l2}) radiative leptonic ($K_{l2\gamma}$) and semileptonic (K_{l3}) decay processes are used to obtain the value of $|V_{us}|$. For leptonic decay $K^+(p) \to l^+(p_l)\nu_l(p_\nu)$ the matrix element involves hadronic matrix element:

$$\langle 0|\bar{s}\gamma_\mu\gamma_5 u|K^-(p)\rangle = if_K p_\mu$$

For semileptonic decay $K^+(p) \to \pi^0 l^+(p_l)\nu_l(p_\nu)$ hadronic matrix element involved is

$$\langle \pi(\vec{p}_\pi)\,|V_\mu|\,K(\vec{p}_K)\rangle = (p_K + p_\pi)_\mu f_+(q^2) + (p_K - p_\pi)_\mu f_-(q^2)$$

Semileptonic decay is more difficult to study but it is important to get alternative information on $|V_{us}|$.

FLAG Review 2024

Flavour Lattice Averaging Group (FLAG)

Snowmass 2013 ➠ present

https://www.usqcd.org/documents/13flavor.pdf and [J. Butler et al, arXiv:1311.1076]

Quantity	CKM element	Present expt. error	2007 forecast lattice error	lattice error	2018 lattice error	2021 FLAG Average
f_K/f_π	$\lvert V_{us}\rvert$	0.2%	0.5%	0.4%	0.15%	0.18 %
$f_+^{K\pi}(0)$	$\lvert V_{us}\rvert$	0.2%	–	0.4%	0.2%	0.18 %
f_D	$\lvert V_{cd}\rvert$	4.3%	5%	2%	$< 1\%$	0.3 %
f_{D_s}	$\lvert V_{cs}\rvert$	2.1%	5%	2%	$< 1\%$	0.2 %
$D \to \pi\ell\nu$	$\lvert V_{cd}\rvert$	2.6%	–	4.4%	2%	0.7 % [from FNAL/MILC, 2212.12648]
$D \to K\ell\nu$	$\lvert V_{cs}\rvert$	1.1%	–	2.5%	1%	0.6 %
$B \to D^*\ell\nu$	$\lvert V_{cb}\rvert$	1.3%	–	1.8%	$< 1\%$	1.7 % [from FNAL/MILC, 2105.14019]
$B \to \pi\ell\nu$	$\lvert V_{ub}\rvert$	4.1%	–	8.7%	2%	~3 %
f_B	$\lvert V_{ub}\rvert$	9%	–	2.5%	$< 1\%$	0.7 % (0.6 % for f_{B_s})
ξ	$\lvert V_{ts}/V_{td}\rvert$	0.4%	2–4%	4%	$< 1\%$	1.3 %
Δm_s	$\lvert V_{ts}V_{tb}\rvert^2$	0.24%	7–12%	11%	5%	4.5 %
B_K	$\mathrm{Im}(V_{td}^2)$	0.5%	3.5–6%	1.3%	$< 1\%$	1.3 %

QED corrections important/dominant source of theory error

CKM matrix from LQCD

precision experimental data on kaon decays determine the product $|V_{us}|f_+(0)$ and the ratio $|V_{us}/V_{ud}| \quad f_{K^\pm}/f_{\pi^\pm}$ (PDG2024):

$$|V_{us}|f_+(0) = 0.21656(35)$$

$$|\frac{V_{us}}{V_{ud}}|\frac{f_{K^\pm}}{f_{\pi^\pm}} = 0.27599(41)$$

$$f_+(0) \equiv f_+^{K^0\pi^-}(0) = f_0^{K^0\pi^-}(0) = \frac{q^\mu \left\langle \pi^-(p') \middle| \bar{s}\gamma_\mu u \middle| K^0(p) \right\rangle}{(M_K^2 - M_\pi^2)}\Bigg|_{q^2\to 0}$$

LQCD results (FLAG):

$f_+(0) = 0.9698(17), \qquad \frac{f_{K^\pm}}{f_{\pi^\pm}} = 1.1934(19)$

produce

$V_{us} = 0.22328(58), \qquad |\frac{V_{us}}{V_{ud}}| = 0.23126(50)$

unitarity: $|V_u|^2 = 0.9820(65)$, i.e. $\approx 3\sigma$ deviation

Determining V_{ud} and V_{us}

$K \to \pi \ell \nu$

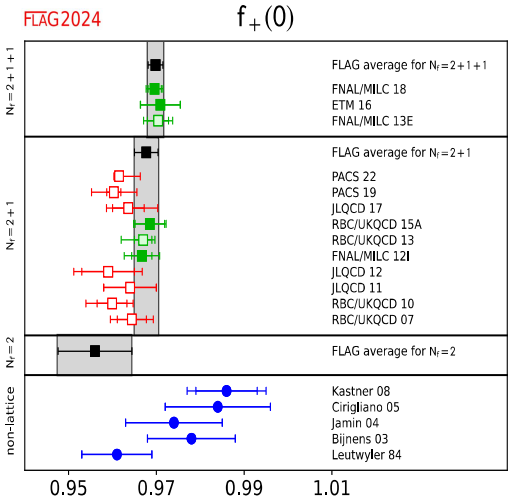

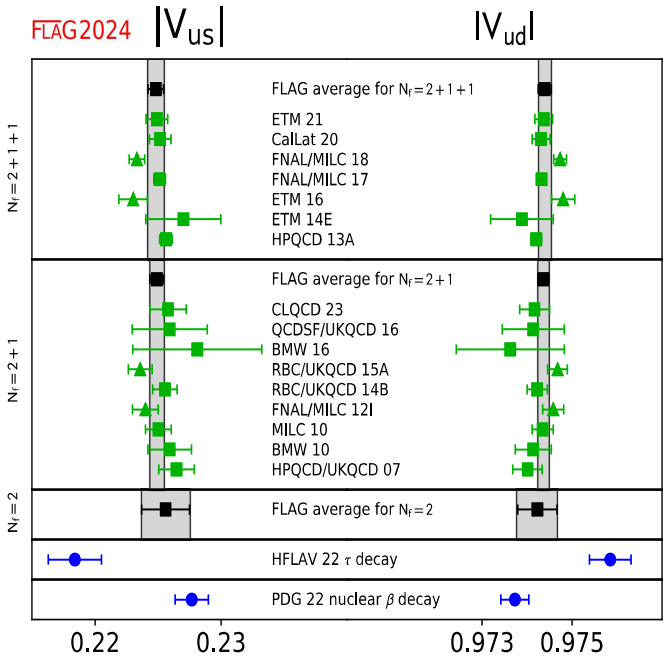

$K \to \ell \nu / \pi \to \ell \nu$

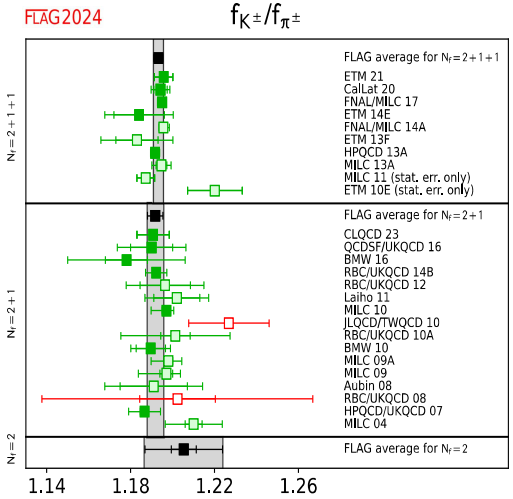

- ✓ different gauge ensembles, fermion and gauge actions
- ✓ different leading systematics
- ✓ independent collaborations

- (✓) "historically" isospin symmetric limit only
- (✓) separation between isoQCD and QED+QCD not uniquely defined

Leptonic radiative decay

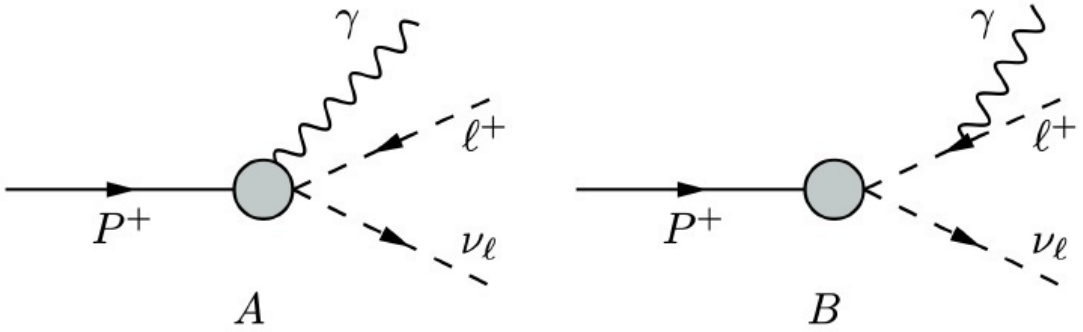

For the radiative decay $P^+ \to \ell^+ \nu_\ell \gamma$, the photon is emitted either from the initial-state meson (Diagram A) or from the final-state lepton (Diagram B). The diagrams correspond to the two terms in $\mathcal{M}^\mu$

$$i\mathcal{M}[P \to \ell\nu_\ell\gamma] = -\frac{G_F e V_{\rm CKM}}{\sqrt{2}} \epsilon_\mu(k,\lambda) \mathcal{M}^\mu(k, p_\ell, p_{\nu_\ell}),$$

$$\mathcal{M}^\mu(k, p_\ell, p_{\nu_\ell}) = f_P L^\mu(k, p_\ell, p_{\nu_\ell}) - H_M^{\mu\nu}(k,p)\, l_\nu(p_\ell, p_{\nu_\ell}).$$

- search for new-physics signals
- alternative determination of the CKM matrix elements
- powerful probes of the mesonic structure

Leptonic radiative decay

1) RBC/UKQCD lattice QCD collaboration,
'Lattice Calculation of Light Meson Radiative Leptonic Decays' e-Print: 2510.26993 [hep-lat]
$P \to l\nu_l\gamma \quad (P = \pi, K)$ Domain wall fermion action

Ensembles	a^{-1}[GeV]	$L^3 \times T$	m_π/MeV	m_K/MeV	$N_{\rm conf}$
48I	1.730(4)	$48^3 \times 96$	139.55(19)	499.21(24)	112
64I	2.359(7)	$64^3 \times 128$	139.18(14)	507.98(35)	119
64I-pq	2.359(7)	$64^3 \times 128$	135.14(19)	496.50(81)	31

- for $\pi \to e\nu_e\gamma$ agreement with the PIBETA collaboration (PSI)
- for $K \to e\nu_e\gamma$ results are consistent with the KLOE (Frascati) data but exhibit a 1.7σ tension with E36 (J-PARC)
- for $K \to \mu\nu_\mu\gamma$ results confirm previously observed discrepancies between lattice results and the ISTRA/OKA measurements at large photon energies, and with the E787 (AGS, BNL) results at large muon–photon angles.

Leptonic radiative decay

2) Extended Twisted Mass Collaboration
'Kaon radiative leptonic decay rates from lattice QCD simulations at the physical point'
Phys.Rev.D 111 (2025) 11, 114523 (e-Print: 2504.08680 [hep-lat])
$N_f = 2 + 1 + 1$ flavors, Wilson-clover twisted mass fermion action
- directly at physical light and strange quark masses
- finite-size effects are carefully investigated using lattices with $L = 3.8$fm to $L = 7.7$ fm
- the continuum extrapolation is based on three lattice spacings in the range $a \in [0.058, 0.08]$ fm.

$$R_\gamma = \frac{Br[K^- \to e^- \bar{\nu}_e \gamma]}{Br[K^- \to \mu^- \bar{\nu}_\mu \gamma]} = 1.84(12)10^{-5}, \qquad E_\gamma > 10\ MeV, \quad p_e > 200\ MeV$$

Leptonic radiative decay

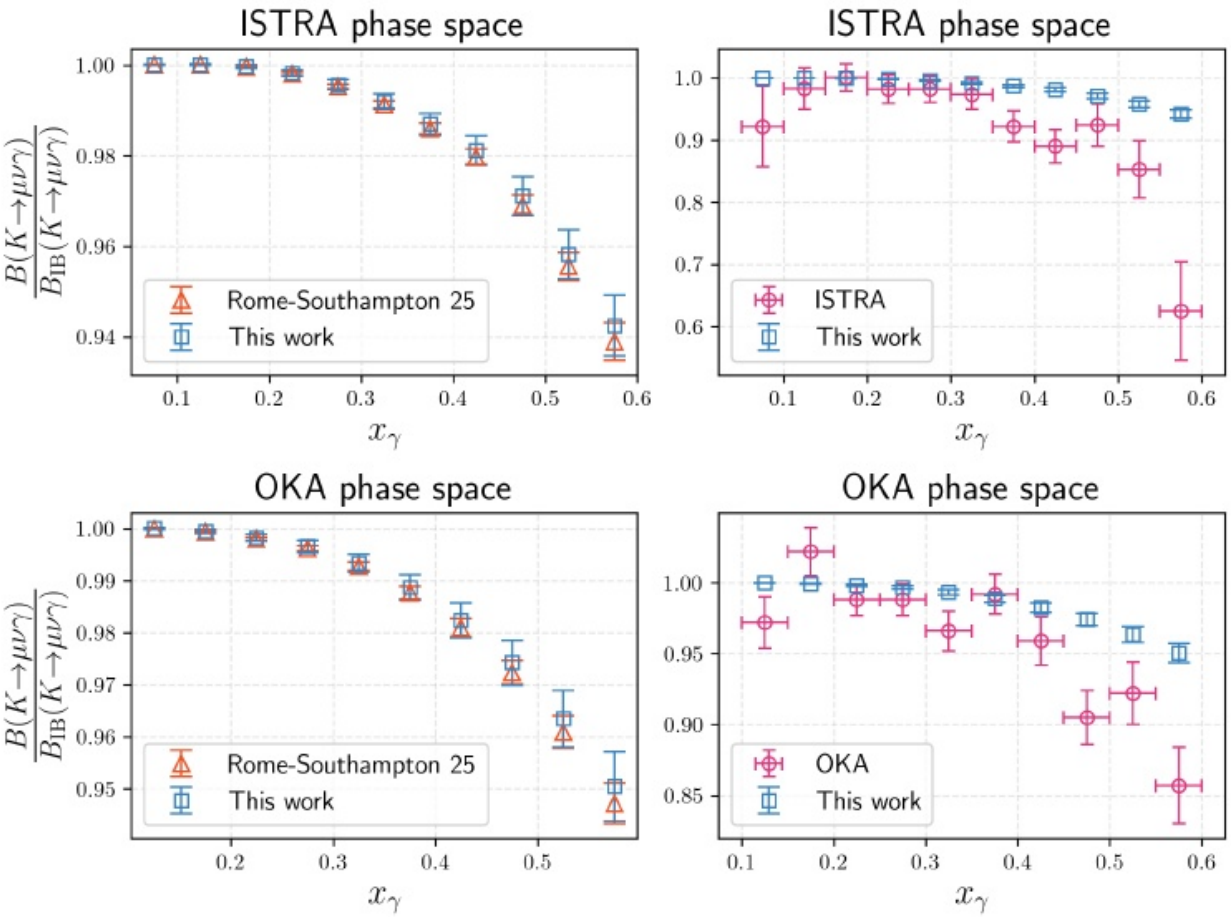

Continuum extrapolated values of the ratio $B(K \to \mu\nu_\mu\gamma)/B_{\rm IB}(K \to \mu\nu_\mu\gamma)$ in the ISTRA and OKA phase-space regions. For comparison, the results from lattice calculation of Ref. [14] and the ISTRA and OKA experimental measurements [18, 19] are also shown.

Conclusions

- Благодаря впечатляющему развитию вычислительных ресурсов и прогрессу в теоретических методах и алгоритмах, решеточная КХД теперь способна давать очень точные и надежные предсказания для широкого спектра адронных величин и предоставляет возможность обнаруживать даже относительно небольшие физические эффекты за пределами Стандартной модели.
- Важно, что различные формулировки действия решеточной КХД и различные методы вычисления физических величин, приводящие, соответственно, к различным систематическим неопределенностям, дают результаты, которые согласуются друг с другом в пределах полученных погрешностей. Это дает уверенность в корректности оценок систематических ошибок и, соответственно, в надежности результатов.